American Mineralogist, Volume 89, pages 204–210, 2004

Halite-sylvite thermoelasticity

DAVID WALKER,[1,*] PRAMOD K. VERMA,[2] LACHLAN M.D. CRANSWICK,[3,†] RAYMOND L. JONES,[4] SIMON M. CLARK,[4,5] AND STEPHAN BUHRE[6]

[1]Lamont-Doherty Earth Observatory and Department of Earth and Environmental Sciences, Columbia University, Palisades, New York 10964, U.S.A.
[2]Department of Geology, Chhatra Marg, University of Delhi, Delhi-110007, India
[3]CCP14—School of Crystallography, Birkbeck College, Malet Street, Bloomsbury, WC1E 7HX, London, U.K.
[4]CLRC, MSL, Daresbury Laboratory, Warrington WA4 4AD, U.K.
[5]Advanced Light Source, LBNL, MS 80-101, 1 Cyclotron Road, Berkeley, California 94720, U.S.A.
[6]Institut fuer Mineralogie, J.W. Goethe-Universitaet, Senckenberganlage 28, 60054 Frankfurt, Germany

ABSTRACT

Unit-cell volumes of four single-phase intermediate halite-sylvite solid solutions have been measured to pressures and temperatures of ~28 kbar and ~700 °C. Equation-of-state fitting of the data yields thermal expansion and compressibility as a function of composition across the chloride series. The variation of the product $\alpha_0 \cdot K_0$ is linear (ideal) in composition between the accepted values for halite and sylvite. Taken separately, the individual values of α_0 and K_0 are not linear in composition. α_0 shows a maximum near the consolute composition ($X_{NaCl} = 0.64$) that exceeds the value for either end-member. There is a corresponding minimum in K_0. The fact that the $\alpha_0 \cdot K_0$ product is variable (and incidentally so well behaved as to be linear across the composition series) reinforces the significance of the complementary maxima and minima in α_0 and K_0 (significantly, near the consolute composition). These extrema in α_0 and K_0 provide an example of intermediate properties that do not follow simply from values for the end-members.

Cell volumes across this series show small, well-behaved positive excesses, consistent with K-Na substitution causing defects through lattice mismatches. Barrett and Wallace (1954) showed maximum defect concentrations in the consolute region. Defect-riddled, weakened structures in the consolute region are more easily compressed or more easily thermally expanded, providing an explanation for our observed α_0 and K_0 variations. These compliant, loosened lattices should resist diffusive transfer less than non-defective crystals and, hence, might be expected to show higher diffusivities. Tracer diffusion rates are predicted to peak across the consolute region as exchange diffusion rates drop to zero.

INTRODUCTION

Physical behavior of a particular structure type depends upon the composition of the material in that structure. Halite (Bl NaCl) and sylvite (Bl KCl) are known to have different volumes, V, compressibilities, β, bulk moduli, K (=1/β), and thermal expansions, α. These two chlorides both have been investigated by simultaneous heating and compression so that it is known that the ratio α/β (= $\alpha \cdot K$) is constant within the stability field of each chloride and is significantly different between them. Boehler and Kennedy (1980) showed that $\alpha_0 \cdot K_0 = 0.0286 = \alpha \cdot K$ for halite. (α is thermal expansion, α_0 is ambient P-T thermal expansion, K is the bulk modulus, and K_0 is the ambient P-T bulk modulus.) Walker et al. (2002b) recently showed from high-temperature-pressure equation-of-state fitting that $\alpha_0 \cdot K_0 = 0.0195$ for sylvite. For both halite and sylvite, the α_0 and K_0 values derived from simultaneous P-T measurements are in agreement with α_0 and K_0 from independent ambient P-T measurements.

Most geological materials problems deal with complex solutions rather than the pure end-member compositions for which physical property information is more commonly available. It is important to know how physical properties vary with composition across solution series to predict the values for intermediate compositions on the basis of end-members. First-order properties such as volume can show a complex and fascinating range of behaviors across different solution series (e.g., Newton and Wood 1980). Volume can behave ideally, show positive excesses, negative excesses, or sigmoidal patterns. We investigated the derivatives (α and K) of the monotonically increasing volumes in the Na-K chloride solution to see whether α and K across the series had a simple relation to the end-members as do the volumes themselves. This is the sort of information needed to decide whether, for instance, the thermal expansion of Mg-Fe lower-mantle magnesiowüstites is reasonably approximated by a linear combination of α values for periclase and wüstite, or is even bounded by the end-member values of α (or β). Compositional, thermal, and compressive cross-derivatives are also of interest in their own right for evaluating mineral energetics.

EXPERIMENTAL ASPECTS

Four mixed chloride solutions between KCl and NaCl were prepared by combination of weighed powders of reagent KCl and NaCl fired at 450 °C. The mechanically mixed powders were melted to form a uniformly thin fluid in a Pt

* E-mail: dwalker@ldeo.columbia.edu
† Present address: Neutron Program for Materials Research (NPMR), National Research Council (NRC), Building 459, Station 18, Chalk River Laboratories, Chalk River, Ontario K0J 1J0, Canada.

crucible at 850–900 °C and quenched by removal from the furnace to cool rapidly in air. Ensuing rapid crystallization produced a complex mixed chloride assemblage of heterogeneous grain size and composition from different generations of dendrites. This assemblage was crushed and ground with BN powder and refired at about 600 °C to promote homogeneity and to dehydrate. BN retards grain-size ripening and X-ray signal loss at *T-P*. The resulting powder produced at Lamont-Doherty Earth Observatory (LDEO) in the U.S. was stored in parafilm-wrapped glass vials for transport to the Daresbury Lab in the U.K.

Compositions achieved by this synthesis may not exactly match the targets attempted. The melting step caused visible fuming. Therefore, spot checks of the composition of experimental products were performed by electron microprobe. Because of grain-scale heterogeneity, probe analysis was done in raster mode with a large number of rasters (50–140) averaged to reconstruct the bulk composition. Within measurement uncertainty, the spot checks reported in Table 1 match the target compositions.

At the Daresbury Lab, the powder prepared at LDEO was packed into the cylindrical cavity on one side of an S (Pt10Rh) thermocouple that bisected the length of a 5 mm inner diameter (ID) graphite furnace tube within a 12 mm truncated edge length octahedral pressure medium. The cavity on the other side of the thermocouple was filled with NaCl, which served as the experimental pressure standard, with admixed BN. As soon as possible after loading the mixed chlorides, the assembly of anvils and pressure medium was inserted between the driving wedges of the octahedral/cubic multi-anvil pressure-temperature device on Station 16.4 of the CLRC Daresbury Lab Synchrotron Radiation Source (Clark 1996) and pressurized. Alternate X-ray illumination of the NaCl then the mixed chloride at a series of pressures and temperatures provided in-situ X-ray diffraction (XRD) spectra from which phase volumes could be computed at known *T* (from the thermocouple) and *P* (from the NaCl). Details of the press, X-ray beam, detector, pressure calibration, and operating procedures may be found in Johnson et al. (2001), and Walker et al. (2002a, 2002b), the present procedures most closely resembling those of Walker et al. (2002b). Diffraction data were taken from an energy-dispersive detector calibrated at least daily for energy against a glass prepared to show fluorescences of Ge, Mo, Sn, Ba, W, and Pb (Walker et al. 2000) and for detector angle (6.6–6.8 °2θ) against NBS Silicon 620b. Spectra were fit with XFIT and unit cells refined with UNITCELL (Coelho and Cheary 1997; Holland and Redfern 1997). The cell volumes are listed in Table 2.

The chlorides are hygroscopic, and the storage and drying procedures were not completely effective at delivering a rigorously dehydrated starting material to the press for *P-V-T* study. This situation was evident during unloading the experiments when rust-like stains were found on the stainless steel endcaps, presumably corrosion from the escape of a small amount of brine. This undesirable complication is not necessarily a catastrophe. The amount of brine did not cause alteration of the bulk composition from the target composition in those two compositions spot checked (Table 1). And trace moisture may have promoted pressure relaxation of the samples.

One of the principal challenges of this study was to achieve and recognize single-phase assemblages so that the single phase measured can be assured of having the bulk composition of the experiment. Two complications intruded. At pressures above 20 kbar, the more K-rich solutions produced a K-rich phase with the B2 structure as well as a more Na-rich B1-structured chloride. Until a comprehensive equation of state (EOS) for B1-structured Na-KCl solutions is developed, the phase compositions of polyphase assemblages cannot be decoded from their X-ray parameters and *P* and *T* alone. Such two-phase experimental observations await interpretation.

The second circumstance impeding the observation of single-phase assemblages is the well-known solvus between halite and sylvite. Nacken (1918),

TABLE 1. Halite-Sylvite physical properties with composition

X(NaCl)	V_0 * Å³/cell Z = 4	K_0 † kbar	±	α_0 /°C	±	$\alpha_0 \cdot K_0$ kbar/°C	±
0.00	249.05	175	6	0.000111	0.000002	0.0195	0.0005
0.20‡	236.48	193	13	0.000109	0.000005	0.0211	0.0011
0.40	221.90	192	5	0.000123	0.000002	0.0236	0.0004
0.60	207.96	197	15	0.000126	0.000006	0.0249	0.0013
0.80§	193.78	219	10	0.000123	0.000004	0.0269	0.0009
1.00	179.34	238	||	0.000120	||	0.0286	||

* From Barrett and Wallace (1954).
† For $K_0' = (5)$.
‡ Spot checks of two experiments: $X_{NaCl} = 0.21 \pm 0.02, 0.19 \pm 0.02$.
§ Spot checks of three experiments: $X_{NaCl} = 0.80 \pm 0.02, 0.82 \pm 0.02, 0.81 \pm 0.02$.
|| From Birch (1986).

TABLE 2. *P-V-T* data for KCl-NaCl Single-phase mixtures

Comp.	File no.	*T* (C)	*P* (Kb)	±	*V* cell (Å³)	±
$K_{10}Na_0$	msl515031	25	0.0	0.0	248.61	0.26
[Sylvite]	r57689	36	0.4	0.1	249.89	0.03
	msl515032	100	0.0	0.0	251.50	0.22
	r57797	100	1.9	0.2	248.18	1.02
	r57761	100	3.9	0.1	245.43	0.99
	r57749	100	8.6	0.2	239.91	0.49
	r57701	100	15.0	0.5	233.44	0.26
	msl515033	200	0.0	0.0	254.37	0.27
	r57793	200	3.1	0.2	248.25	0.94
	r57765	200	5.5	0.2	245.23	0.96
	r57745	200	10.2	0.0	240.49	0.73
	r57705	200	15.7	0.4	234.55	0.14
	msl515034	300	0.0	0.0	257.62	0.31
	r57769	300	6.7	0.2	246.28	0.93
	r57741	300	11.7	0.1	239.30	0.63
	r57709	300	16.2	0.3	236.43	0.11
	msl515035	400	0.0	0.0	260.72	0.41
	r57789	400	6.1	0.2	250.19	0.93
	r57773	400	8.6	0.2	247.63	1.13
	r57737	400	13.4	0.1	241.01	0.54
	r57713	400	16.5	0.3	238.12	0.13
	msl515036	500	0.0	0.0	264.86	0.44
	r57777	500	8.9	0.1	248.38	0.97
	r57733	500	15.0	0.1	241.68	0.49
	r57717	500	17.1	0.2	239.78	0.09
	msl515037	600	0.0	0.0	270.14	0.61
	r57781	600	9.9	0.1	251.14	0.59
	r57721	600	17.3	0.1	242.28	0.23
	r57725	600	17.3	0.1	241.59	0.57
K_9Na_1	b&w	25	0.0	0.0	242.35	
	als3k90	500	0.0	0.0	257.91	0.32
	als2k90	600	0.0	0.0	262.49	0.16
K_8Na_2	b&w	23	0.0	0.0	236.48	
	als11k80	300	0.0	0.0	244.34	0.57
	r55633	300	3.6	0.5	239.48	0.18
	als10k80	350	0.0	0.0	245.83	0.40
	r55501	350	17.2	0.2	224.31	0.12
	als9k80	400	0.0	0.0	247.44	0.34
	r55629	400	5.2	0.4	240.28	0.11
	r55493	450	19.0	0.2	224.28	0.06
	r53261	475	12.1	0.2	234.59	0.06
	als7k80	500	0.0	0.0	251.33	0.13
	r55617	500	7.0	0.4	241.37	0.09
	r55577	500	9.6	0.6	236.99	0.03
	r53253	500	12.3	0.1	234.84	0.30
	r55377	500	15.0	0.2	230.58	0.11
	r53197	500	18.0	0.2	229.09	0.20
	als6k80	550	0.0	0.0	253.30	0.25
	r55589	550	10.1	0.4	238.32	0.11
	r53249	550	13.3	0.1	234.99	0.13
	r55373	550	16.0	0.2	230.89	0.10
	r53201	550	18.1	0.2	229.49	0.26
	als5k80	600	0.0	0.0	255.85	0.24
	r55593	600	7.5	0.6	238.89	0.16
	r55613	600	7.5	0.6	241.43	0.28
	r53237	600	14.0	0.2	235.53	0.19
	r55369	600	17.0	0.2	231.15	0.12
	r53205	600	18.1	0.2	230.35	0.24
	als3k80	650	0.0	0.0	257.88	0.32
	als4k80	650	0.0	0.0	258.64	0.20
	r55597	650	7.7	0.6	240.29	0.19
	r53233	650	14.6	0.2	236.07	0.15
	r53217	650	18.6	0.2	231.94	0.16
	r55601	700	8.0	0.6	241.39	0.14
	r53221	700	15.6	0.2	235.81	0.10
	r55365	700	19.0	0.2	231.71	0.21
K_7Na_3	b&w	25	0.0	0.0	228.78	
	als4k70	500	0.0	0.0	244.83	0.57
	als3k70	550	0.0	0.0	247.23	0.41
	als2k70	600	0.0	0.0	249.59	0.47
	als1k70	650	0.0	0.0	252.36	0.15
K_6Na_4	b&w	25	0.0	0.0	221.90	
	r54811	400	15.0	0.4	216.25	0.16
	r54935	450	8.8	0.5	223.47	0.15
	r54883	450	8.9	0.4	223.54	0.22
	r54807	450	15.7	0.4	216.44	0.14
	als13k60	500	0.0	0.0	237.83	0.15

TABLE 2.—*continued*

Comp.	File no.	*T* (C)	*P* (Kb)	±	*V* cell (Å^3)	±
	r54907	500	9.8	0.5	223.50	0.15
	r54927	500	9.8	0.5	223.99	0.06
	r54879	500	10.1	0.4	223.91	0.21
	r52113	500	11.9	0.1	220.87	0.55
	r54803	500	16.5	0.4	216.71	0.11
	als12k60	550	0.0	0.0	240.18	0.21
	r54875	550	11.2	0.4	224.59	0.13
	r52105	550	12.6	0.2	221.26	0.44
	r54795	550	17.3	0.4	216.88	0.08
	als11k60	600	0.0	0.0	242.91	0.60
	als5k60	600	0.0	0.0	242.26	0.38
	als6k60	600	0.0	0.0	242.45	0.58
	r54911	600	11.5	0.5	224.17	0.19
	r54863	600	12.4	0.4	223.55	0.10
	r52081	600	15.4	0.1	220.18	0.13
	r54827	600	18.8	0.3	216.54	0.12
	als9k60	650	0.0	0.0	245.33	0.28
	als7k60	650	0.0	0.0	245.31	0.46
	als8k60	650	0.0	0.0	245.25	0.45
	als10k60	650	0.0	0.0	245.62	0.12
	r54867	650	12.4	0.4	223.84	0.25
	r52085	650	15.1	0.2	220.64	0.20
	r54835	650	19.6	0.3	216.45	0.14
	r54783	650	19.6	0.4	216.67	0.10
	r54871	700	12.4	0.4	225.57	0.14
	r52097	700	15.3	0.1	222.26	0.32
	r54787	700	19.7	0.4	217.45	0.09
K_5Na_5	b&w	25	0.0	0.0	214.96	
	als4k50	500	0.0	0.0	229.92	0.40
	als3k50	550	0.0	0.0	232.03	0.44
	als2k50	600	0.0	0.0	234.43	0.60
	als1k50	650	0.0	0.0	237.16	0.11
K_4Na_6	b&w	25	0.0	0.0	207.96	
	r54490	400	16.9	0.3	200.18	0.09
	r57084	450	7.6	0.2	212.48	0.38
	r57152	450	15.9	0.1	203.69	0.15
	r57212	450	20.6	0.4	199.95	0.06
	als6k40	500	0.0	0.0	222.80	0.09
	r57080	500	8.6	0.2	212.94	0.40
	r54394	500	12.2	0.3	206.26	0.00
	r57148	500	16.9	0.1	203.95	0.19
	r54486	500	18.6	0.3	200.75	0.10
	als5k40	550	0.0	0.0	225.12	0.07
	r57076	550	9.6	0.2	213.61	0.36
	r54390	550	13.2	0.3	206.67	0.08
	r57144	550	17.8	0.1	204.17	0.17
	r57204	550	22.9	0.4	200.36	0.05
	als4k40	600	0.0	0.0	227.50	0.17
	r54382	600	14.1	0.3	206.91	0.05
	r54414	600	14.1	0.4	206.65	0.13
	r54426	600	14.1	0.4	206.51	0.11
	r53017	600	18.4	0.1	203.54	0.06
	r54482	600	20.4	0.3	201.21	0.10
	r54470	600	21.2	0.3	199.98	0.08
	r53021	625	18.3	0.2	203.74	0.13
	als3k40	650	0.0	0.0	229.94	0.24
	r57068	650	11.5	0.2	215.04	0.07
	r54366	650	15.9	0.2	206.67	0.06
	r53025	650	18.2	0.2	204.53	0.10
	r57136	650	19.6	0.1	205.26	0.26
	r57196	650	25.2	0.4	200.74	0.04
	r53029	675	18.1	0.2	204.90	0.13
	r57064	700	12.5	0.2	215.58	0.21
	r54370	700	16.0	0.2	207.86	0.08
	r53053	700	16.3	0.1	207.86	0.24
	r53041	700	18.0	0.2	206.54	0.28
	r57132	700	20.6	0.1	205.37	0.27
	r54474	700	22.1	0.3	201.80	0.08
	r57240	700	26.0	0.5	200.88	0.11
	r53049	750	17.2	0.2	207.85	0.11
K_3Na_7	b&w	25	0.0	0.0	200.90	
	als6k30	508	0.0	0.0	215.08	0.34
	als5k30	550	0.0	0.0	217.11	0.17
	als4k30	600	0.0	0.0	219.37	0.31
	als3k30	650	0.0	0.0	221.71	0.31
K_2Na_8	b&w	25	0.0	0.0	193.78	
	r56329	350	11.8	0.1	191.40	0.18

TABLE 2.—*continued*

Comp.	File no.	*T* (C)	*P* (Kb)	±	*V* cell (Å^3)	±
	r56361	350	12.4	0.1	191.25	0.07
	r56417	350	21.0	0.1	184.78	0.03
	r56325	400	12.6	0.3	191.86	0.08
	r56413	400	21.9	0.2	185.01	0.03
	r56321	450	13.4	0.3	192.24	0.10
	r56409	450	22.8	0.2	185.29	0.04
	als9k20	500	0.0	0.0	207.78	0.50
	r56317	500	14.2	0.3	192.69	0.04
	r53621	500	15.8	0.3	191.35	0.09
	r56405	500	23.6	0.2	185.62	0.09
	als8k20	550	0.0	0.0	210.08	0.23
	r56313	550	15.0	0.3	193.05	0.10
	r53693	550	17.6	0.2	190.27	0.05
	r56401	550	24.5	0.2	185.89	0.08
	r56429	550	25.1	0.2	185.10	0.33
	r56437	550	25.1	0.2	185.11	0.42
	r56453	550	25.2	0.0	185.51	0.10
	als7k20	600	0.0	0.0	212.03	0.57
	r56309	600	15.8	0.3	193.46	0.10
	r56281	600	17.4	0.1	191.66	0.06
	r53633	600	17.7	0.1	191.68	0.15
	r56397	600	25.4	0.2	186.13	0.09
	r53573	610	19.6	0.2	188.24	0.37
	r53581	620	19.4	0.3	189.54	0.36
	r56289	625	17.5	0.1	192.43	0.04
	r53585	630	19.2	0.3	189.94	0.40
	r53589	640	19.0	0.3	190.46	0.30
	als6k20	650	0.0	0.0	214.39	0.41
	r56293	650	17.5	0.1	193.00	0.12
	r56357	650	18.2	0.2	192.94	0.04
	r56373	650	18.2	0.2	192.74	0.16
	r53593	650	18.8	0.3	190.86	0.30
	r56393	650	26.3	0.2	186.40	0.06
	r56381	650	26.8	0.2	186.09	0.07
	r53601	675	19.0	0.3	192.03	0.15
	r56297	700	17.5	0.1	194.08	0.09
	r56385	700	27.2	0.1	186.49	0.05
	r56441	700	28.2	0.2	186.01	0.08
K_1Na_9	b&w	25	0.0	0.0	186.59	
	als3k10	550	0.0	0.0	201.56	0.25
	als2k10	600	0.0	0.0	203.71	0.12
	als1k10	650	0.0	0.0	205.71	0.30
K_0Na_{10} [Halite]	msl416031	25	0.0	0.0	179.42	0.16
	msl416032	100	0.0	0.0	180.65	0.16
	msl416033	200	0.0	0.0	183.73	0.18
	msl416034	300	0.0	0.0	185.89	0.15
	msl416035	400	0.0	0.0	188.33	0.14
	msl416036	500	0.0	0.0	191.42	0.17
	msl416037	600	0.0	0.0	194.26	0.25

Notes: b&w = data from Barrett and Wallace (1954); mslxxxxxx file nos run on rotating anode at MSL Daresbury; r5xxxxx file nos run on Daresbury Station 16.4; alsxkxx file nos run on ALS Station 7.3.3.

Barrett and Wallace (1954), and Thompson and Waldbaum (1969) disagree only on the exact details of the shape of an extensive temperature-composition (*T-X*) region of phase separation that was encountered in these experiments. It was not an experimental blunder to have stumbled into such complications. We purposely chose a compressible system with a known solvus hoping to see interesting effects on the composition-dependent EOS and perhaps see the details of the shape and pressure dependence of the solvus. This work is in progress.

The power of the in situ XRD technique is that the complications of intrusive phase separation can be recognized without the ambiguities of examination of quench products. We have ample evidence from real-time observations by in situ XRD for the rapidity of solid-state reactions in this system that would make it difficult to interpret observations on quench products.

A typical data collection sequence with an intermediate K-Na chloride would be to load it into the on-line press and do unpressurized and unheated illuminations of the NaCl standard and the mixed chloride. The V_0 measured for NaCl provides the reference volume for calculating sample pressure with EOS BE_2 for NaCl given by Birch (1986). The spectrum observed for the mixed chloride usually showed broad peaks or a range of peaks consistent with the presence of several different K-Na chlorides either grown during the quench following the melting to a homogeneous liquid, or grown on quench following the final baking. Cold pressurization to

10–20 Kbar was followed by re-illumination of each half of the charge to assess the pressure and state of the mixed chloride. Usually, little change in the mixed chloride was observed until heating to 250–300 °C. At that point, the spectra began to resolve themselves better into 2 populations of chloride peaks: one K-rich and one Na-rich. By 400 °C, the two groups of peaks were quite well-established and could be seen to converge in energy upon each other with further heating or to separate upon cooling on time scales of 10–15 min. Depending on bulk composition, 450–550 °C was sufficient to homogenize the K-Na chloride to a single set of B1 peaks. These spectra are then the first to be of any use to the present study, and to give the cell parameter of a single-phase mixed chloride with the known bulk composition. Heating and illumination of the NaCl and mixed chloride continued to perhaps 700 °C, these spectra also being useful for the EOS with the virtue that the alternate illuminations of NaCl provided good determination of sample pressure. At this point, the temperature was rapidly dropped in 50 °C increments and quick 2–3 min spectra of the single-phase mixed chloride were collected at each temperature step. No time-consuming raising and lowering of the press to hit the NaCl pressure standard was undertaken because the kinetics of exsolution were quite rapid. We wished to extend the temperature range of the *P-V-T* information on each bulk composition by collecting single phase spectra down in temperature into the phase separation region as far as possible. The metastable single-phase compositions could be observed for a limited temperature-time (*T-t*) window. Typically, by the time the 400 or 350 °C step was reached, there was a sudden dramatic exsolution event that could be watched spectrally on-screen in real time. The major reflections of the spectrum, (200) and (220), were not seen to split into pairs that migrated in energy away from the single-phase reflection as might be expected in a spinodal decomposition mechanism. Instead, satellite peaks on either side of the original single reflection suddenly appeared and grew as the original reflection diminishes. None of the three reflections showed applicable energy shift (*d*-spacing shift) during the process, which takes only minutes to complete. This observation suggests a nucleation and growth mechanism of reaching equilibrium, rather than metastable spinodal decomposition. Once the exsolution was complete, the NaCl was re-illuminated to establish the pressure at the end of the down-temperature step sequence. Pressure always falls in this sequence through loss of thermal pressure at constant press force. Johnson et al. (2001) showed that the characteristics of the Daresbury Station 16.4 press and gasket system resemble those of a constant volume device at constant press force, especially after the first heating cycle. Thus, the heating and rapid step-wise cooling cycles at constant press force do produce pressure drops. We reckon the pressure at intermediate steps between the initial and final ones, where NaCl pressure is known, by interpolation. To do otherwise and pause to take an NaCl pressure at each temperature step would cause us to be unable to collect the metastable single-phase, low-temperature information. Even without pausing to take NaCl pressure, we did not succeed in collecting single-phase *P-V-T* information below 350 °C for any of the mixed chlorides. Single-phase cell volumes are given in Table 2 and Figure 1.

Additional data were collected at ambient pressure for a series of mixed chlorides at 10% increments of the fraction of NaCl, X_{NaCl}, between halite and sylvite at temperatures above the solvus and up to 650 °C. The end-members halite and sylvite were measured in the heating stage of the rotating anode X-ray source of the Materials Science Lab (MSL) of the Daresbury Laboratory. Reagent NaCl and KCl were ground with MgO and placed in quartz glass capillary tubes for insertion into the heating stage.

Temperatures were monitored and controlled with chromel-alumel (type K) thermocouples. The XRD spectra from Cu$K\alpha$ radiation were collected on an INEL position-sensitive detector. The 3 MgO peaks in the spectrum were used to calibrate the detector response for each spectrum. The 4–6 peaks collected at each temperature from the end-member chlorides were fit and regressed using similar procedures as for the Station 16.4 data. The intermediate compositions were measured at the Advanced Light Source (ALS) at the Lawrence Berkeley National Laboratory using the heating stage from MSL Daresbury temporarily installed on Station 7.3.3. For the ALS 7.3.3 configuration, the admixed MgO was used as an internal standard to compute the sample to the MAR 345 image plate distance for each spectrum (about 184 mm). Once the image plates were integrated, cell parameters were recovered from peak fitting and regression using a known input radiation wavelength of 1.1169 Å. The results of these ambient pressure determinations are recorded in Table 1 and Figure 2.

For each of 4 bulk compositions at 20% intervals between KCl and NaCl, the *P-V-T* data for single-phase observations were tabulated and fit with an EOS of the BE_1 form of Birch (1986). The 500 and 600 °C isotherms and the 500 and 600 °C data for sylvite and the 4 mixed chloride compositions are shown in Figure 1. The fitting procedures followed are given in Walker et al. (2002a, 2002b). For these very modest compressions, no use of K_0' or a BE_2 form of the EOS is warranted.

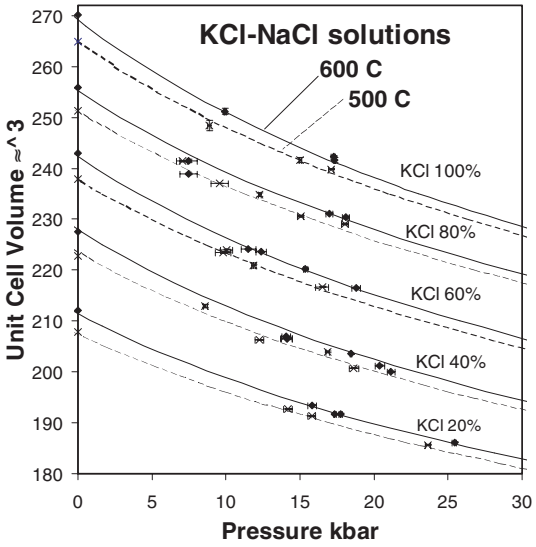

FIGURE 1. Isotherms for sylvite and 4 other single-phase mixed K-Na chlorides. Isotherms are fit to all data of Table 2. Only the data points for 500 and 600 °C are shown individually.

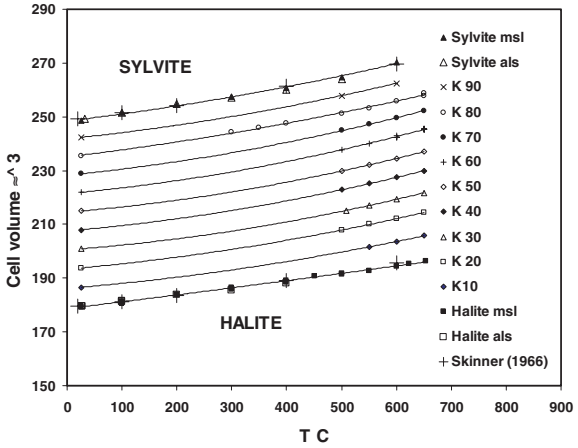

FIGURE 2. *T-V* data for single-phase chlorides. Absence of data at intermediate compositions below 500 °C reflects intrusion of phase separation.

In fact, we did not fit for K_0' with BE_1 but adopted the value of [5] reflecting the fact that insufficient range of compression was encountered with our pressure spacing of observations to fit K_0' reliably. (The use of square brackets indicates an arbitrarily adopted value rather than one generated from fitting the data.) For V_0, we took the values given by Barrett and Wallace (1954). Thus BE_1 fitting of the EOS *P-V-T* observations was an exercise in retrieving α_0 and K_0, which are given for each composition in Table 1 and Figure 3. The fitting was done with and without the ambient pressure data included. The filled diamonds in Figure 3 include the ambient pressure data whereas the triangles (DL only) do not.

RESULTS

The product $\alpha_0 \cdot K_0$ is roughly constant throughout the field of stability of a phase. For instance, B1 KCl has $\alpha_0 \cdot K_0 = 0.0195$, which does not show resolvable variation within B1 stability whereas $\alpha_0 \cdot K_0 = 0.0275$ for B2 KCl is significantly different (Walker et al. 2002b). Yagi (1978) has shown that $\alpha \cdot K$ constancy is only approximate and is less variable for B1 structures than B2.

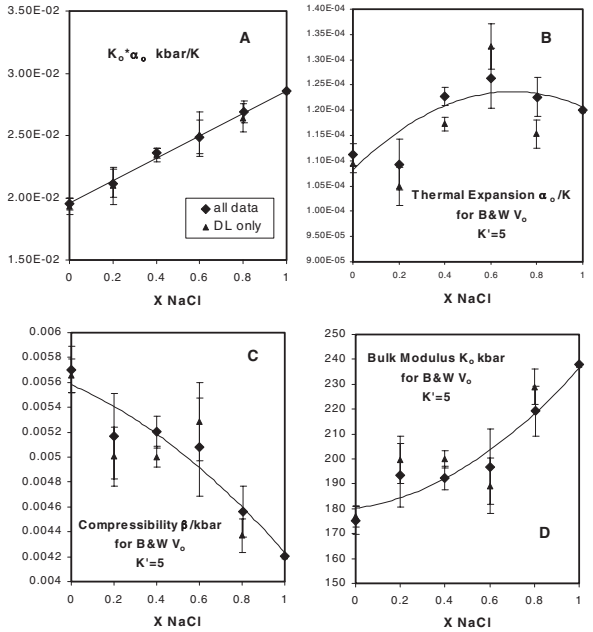

FIGURE 3. Variation of properties as function of X_{NaCl} across the halite-sylvite series. DL+ALS data includes ambient pressure in the fitting procedure using the BE1 equation of Birch (1986). DL data does not include ambient pressure ALS data. Regressions through either grouping are similar; the addition of the ambient pressure data moderates the variation recovered in the variation of fit parameters.

Our fitting procedure with BE_1 does not examine whether or not $\alpha{\cdot}K$ is constant. It is assumed to be so for each phase composition that we fit. But the constant value of the product is not constrained to be anything in particular by the fitting procedure.

The constant $\alpha_0{\cdot}K_0$ fitting procedure adopted for the BE_1 equation is not to be confused with the proposition that α and K are constants. They are not. For instance, the isopleths of Figure 2 show curvature requiring that α increase with T. At the same time, however, K decreases proportionately to keep $\alpha{\cdot}K$ fixed. The fitting procedure evades the need to keep explicit track of the local variations of α and K. In so much as there is real variation of $\alpha(T,P)$ or $K(T,P)$, the values of α and K recovered in the fitting procedure will reflect average values over the domain fit, rather than the ambient α_0 and K_0.

Figure 3A shows the variation in $\alpha_0{\cdot}K_0$ retrieved for the 4 intermediate solutions in KCl-NaCl. They fall on a linear array with the accepted values for KCl (Skinner 1966; Walker et al. 2002b) and NaCl (Birch 1986; after Boehler and Kennedy 1980) as the end-members. No error bars are put on $\alpha_0{\cdot}K_0$ for NaCl because that is the value to which all the rest are tied through the use of $\alpha_0{\cdot}K_0 = 0.0286$ kbar/°C in the NaCl EOS, which serves as the pressure reference. The error bars on KCl from Walker et al. (2002b) are set from the extent of the fitting residuals. They are sufficient to include the α_0 value of Skinner (1966) measured at ambient pressure and the mutually agreeing ambient-temperature K_0 values of Vaidya and Kennedy (1971), Yagi (1978), and Hofmeister (1997). The intermediate composition error bars also are scaled to the residuals in the fitting process, but there is no other study of these compositions with which to compare them. But one does not need to obsess over the error bars to see that the $\alpha_0{\cdot}K_0$ array in Figure 3A is indistinguishable from linear.

The linear $\alpha_0{\cdot}K_0$ array is a very satisfying result. The linearity is consistent with well-behaved data. The extrapolation of the linear array for the intermediate compositions to hit the known values for NaCl and KCl is not preordained by the fitting process, and therefore increases confidence in the reliability of the data. Some bolstering of confidence may be needed after inspection of Figures 3B to 3D. At first glance, one might declare the intermediate composition arrays to resemble noise. In the case of the thermal expansion variations, the noise is not even bounded by the NaCl and KCl end-member values. Such a dark view of the matter probably could be tested best by a more densely populated array of compositions to confirm with what fidelity the observed variations persist, or whether they dissolve into noise. The resources in endurance, patience, and beam time to expand the observational database are currently unavailable. Even so, there are reasons to take a less jaundiced view.

The first is Figure 3A. The $\alpha_0{\cdot}K_0$ array is encouragingly simple and stable. However, this stability may not propagate to the α_0, K_0, or β_0 arrays. Indeed Walker et al. (2002b) showed that very stable $\alpha_0{\cdot}K_0$ fitting solutions for B2 KCl can be achieved even though α_0 and K_0 could individually vary by as much as 50%. This is an unpleasant manifestation of parameter correlation in fitting with the BE_1 form. But Walker et al. (2002b) only achieved this result by treating K_0' and V_0 as free-fitting parameters. In the present application where K_0' is fixed and V_0 is accurately known from the study of Barrett and Wallace (1954), such latitude does not exist and so Figure 3A does provide some encouragement.

A second reason for optimism is that it is possible to obtain a semi-independent check on the fitting fidelity of the thermal expansion variation with composition seen in Figure 3B. The ALS data collected at ambient pressure is a good test data set to examine the compositional dependence of thermal expansion without pressure complications. Figure 4 shows the thermal expansion data of Figure 3B fit from all *P-T* covered by this study in comparison with the ALS and DL-MSL ambient pressure thermal expansions of the chloride series at 500 °C. (Table 3 records the 500 °C thermal expansions obtained by quadratic fit to the *T-V* data in Table 2. Lower and ambient *T* thermal expansions are not available at intermediate compositions because of the intrusion of phase separation.) The broad arch peaking at the consolute composition seen in Figure 3B is also seen in the 500 °C ambient pressure data in Figure 4. The fact that the 500 °C arch is at higher values of thermal expansion reflects the fact that the ambient fitting explicitly fits $\alpha(T)$ and thermal expansion increases with *T*. The arch from Figure 3B did not explicitly fit $\alpha(T)$ but found an average for the *T* domain sampled. The real variation of thermal expansion with *T* is also reflected in the accepted values from Skinner (1966), the ambient and 500 °C values from Skinner (1966) being the large open diamonds and triangles respectively at the compositional limits of the plot for sylvite and halite. The *P-V-T* fitting values fall agreeably between the accepted halite and sylvite values. The discovery of an intermediate composition peak in the thermal expansion in both *P-V-T* and *T-V* data argues for the reality of this maximum.

The third reason for optimism is that fairly plausible physical

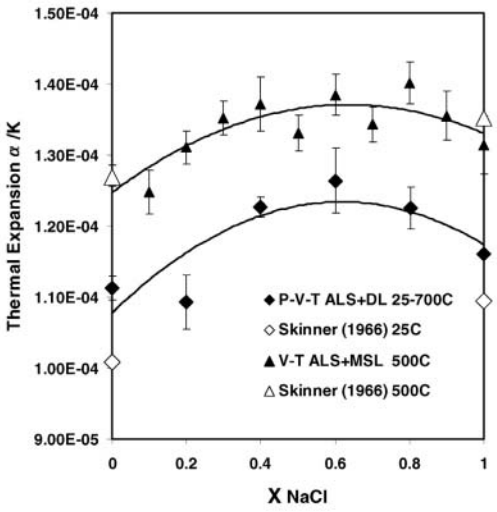

FIGURE 4. Thermal expansion from fitting all *P-V-T* data compared to thermal expansion at 500 °C measured at ambient pressure at ALS and DL-MSL. Both curves show a maximum near the consolute composition.

interpretations of the swings of α_0, β_0, and K_0 along the arrays of Figures 3B to 3D are possible.

DISCUSSION

To a first approximation, Figure 3B of the α_0 variation in the NaCl-KCl series shows a maximum at $X_{NaCl} = 0.6$ superimposed on an otherwise bland transition from one end-member to the other. The consistently positive excess volumes across this series reported by Barrett and Wallace (1954) suggest the accommodation of Na-K size mismatches occurs by introduction of lattice defects. They calculated that up to percent levels of Schottky defects would be required to reconcile the mismatch between their bulk density and lattice parameter measurements. X_{NaCl} = 0.6 is the compositional region shown by Barrett and Wallace (1954) to have the largest population of such defects. (It is also the region of the consolute composition for reasons that make geometric sense. The consolute composition is more Na-rich than K-rich because it is more difficult to substitute a large K for a small Na than the reverse. Thus, the K-Na chlorides provide a good example of the well-known tendency of solvi to lean toward and crest toward the small end-member of the composition series.) Defect-riddled lattices may be expected to be poorer at resisting thermal expansion than their less-defective counterparts. Therefore, we argue the plausibility of finding a maximum in thermal expansion and of finding it at the maximum-defect composition region.

The considerations leading us to expect that a defect-weakened lattice will be more thermally expansible also lead to the expectation that such a lattice will be more compressible. And, indeed, we also see a maximum in the compressibility (or a minimum in the bulk modulus) at this composition $X_{NaCl} = 0.6$ in Figure 3C and 3D.

One might argue that the minimum in K_0 is forced to follow from a maximum in α_0 through the $\alpha_0 \cdot K_0$ = constant constraint of the BE_1 form. But this argument would not be correct because

TABLE 3. Thermal expansion

X_{NaCl}	α (500 °C)	±
1	0.000131	0.000004
0.9	0.000136	0.000003
0.8	0.000140	0.000003
0.7	0.000134	0.000003
0.6	0.000139	0.000003
0.5	0.000133	0.000003
0.4	0.000137	0.000004
0.3	0.000135	0.000002
0.2	0.000131	0.000002
0.1	0.000125	0.000003
0	0.000127	0.000001

there is no constraint from BE_1 fitting that $\alpha_0 \cdot K_0$ has to have a particular value, only that it be a constant for some composition, and perhaps some other constant for some other composition. Thus, to have the α_0 maxima and K_0 minima synchronized across the compositional series is not an artifact of the fitting process. The fact that the $\alpha_0 \cdot K_0$ variation is so smooth, that the α_0 and K_0 extrema are correlated, and correlated at a composition that makes physical sense, all argue for the reality of these observations. They can be checked by further experimentation.

K-NA TRANSFER

Our hypothesis is that the defect-weakened structure in the consolute region is more compressible and expansible than the structures outside the consolute region. The consolute region is known to contain the most defects (Barrett and Wallace 1954). This lattice weakening should have predictable effects on diffusive transport properties, for example, K-Na exchange. Lattice misfits provide favorable activation paths for transfer. In addition, lattices swell locally as atoms make their activated jump to transfer through a constricted lattice. Such swelling is a microscopic analog of macroscopic thermal expansion. Likewise, compressibility is a macroscopic compliance relevant to microscopic activation for transfer. The more compressible a substance, the easier for atoms to squeeze through constricted lattices. Thus, larger thermal expansions and compressibilities are expected to lower resistance to the activation process. The consolute region should be characterized by relatively easy diffusive transfer because the activation barriers are lowered.

Other things being equal, a rise of K-Na exchange rates across the consolute region would be expected from the lowering of the barriers to such exchange. However, other things are not equal because the consolute region is quite special. The consolute region is the one of maximum mismatch requiring the highest temperatures to stabilize a uniform solution. The solvus beneath the consolute region is a manifestation of the structural problems inherent in uniformly mixing non-uniform-sized ions on-site when temperature is not high enough. In the limit of temperature and composition dropping into the solvus, the presence of the separated phases across the limbs of the solvus fixes the chemical potential of KCl (or of NaCl) at zero difference from one limb to the other of the solvus. In the consolute region approaching this limit, the exchange chemical potential is in the process of dropping to zero. Therefore, although the activation barriers to exchange diffusion are diminished by the defective lattice, the chemical potential difference for driving exchange diffusion is also being diminished. In the consolute region, the energetics are set by the defective structure, with the composi-

tional details of the K^+-Na^+ populations making relatively little impact. Thus K^+-Na^+ exchange diffusivities may be expected in the limit to drop to zero. It is possible that they could initially rise if the activation barrier removal kicks in before the driving force disappears. It would be instructive to explore this question experimentally, even though the limiting behavior can be predicted confidently.

No such disappearing driving force problems would hobble tracer diffusion. Na^+ or K^+ isotope imbalances across the solvus and the consolute region would provide a driving force for isotopic exchange that is unaffected by the details of the structural environment or K^+-Na^+ exchange chemical potentials. And yet the rate of isotopic exchange is still sensitive to the structural constraints on the activation process for transfer. $^{39}K/^{41}K$ imbalances will not be redressed unless K^+ can actually move through the lattice. Likewise the dispersal of radioactive ^{22}Na requires Na^+ mobility through the lattice. Thus, we propose that the signature of a defect-induced solvus will be that tracer diffusion rates should show maxima across the consolute region even as exchange diffusivities minimize. If observed, these diffusivity patterns would provide logically consistent support for our interpretation of the thermoelastic anomalies we observe in halite-sylvite.

Concluding remarks

We observed well-behaved linear $\alpha_0 \cdot K_0$ variation across halite-sylvite at the same time we observe maxima and minima in α_0 and K_0 near the consolute composition $X_{NaCl} = 0.64$. We interpret these extrema as manifestations of defect-weakened lattice structure caused by K-Na misfits. We suggest an examination of tracer diffusivity rates for confirmation of this interpretation.

The variation of the thermoelastic parameters across the B1-structured halite-sylvite solid solution series suggests that caution be used in predicting either α_0 or K_0 in complex solutions even if their product $\alpha_0 \cdot K_0$ can be shown to be ideal. This lesson may be applicable to the B1-structured magnesiowüstite oxides. The smaller size mismatch between Mg^{2+} and Fe^{2+} than between K^{1+} and Na^{1+} should render the penalties of the lesson less severe in the oxide series than in the chlorides. Even so, Reichmann et al. (2000) reported difficulties matching measured intermediate elastic constants for Mg-Fe oxides with those interpolated from the values for periclase and wüstite. α_0 and K_0 measurements in the oxide series would be of interest.

Acknowledgments

This work was supported by the U.K. Natural and Environmental Research Council, CLRC Daresbury Lab., and the U.S. National Science Foundation. We thank Abby Kavner for discussion. We appreciate the review comments of two anonymous reviewers. We have benefited from the EPSRC-funded CCP14 project at http://www.ccp14.ac.uk. We thank Jean Hanley, Christine Ra, and Patricia Nobre for technical assistance. The Advanced Light Source is supported by the Director, Office of Science, Office of Basic Energy Sciences, Materials Sciences Division, of the U.S. Department of Energy under contract no. DE-AC03-76SF00098 at Lawrence Berkeley National Laboratory. Lamont-Doherty Earth Observatory contribution no. 6547.

References cited

Barrett, W.T. and Wallace, W.E. (1954) Studies of NaCl-KCl solid solutions. I. Heats of formation, lattice spacings, densities, Schottky defects and mutual solubilities. Journal of the American Chemical Society, 76, 366–369.

Birch, F. (1986) Equation of state and the thermodynamic parameters of NaCl to 300 kbar in the high-temperature domain. Journal of Geophysical Research, 91, 4949–4954.

Boehler, R. and Kennedy, G.C. (1980) Equation of state of sodium chloride up to 32 kbar and 500 °C. Journal of Physics and Chemistry of Solids, 41, 517–523.

Clark, S.M. (1996) A new energy dispersive powder diffraction facility at the SRS. Nuclear Instruments and Methods in Physics Research, A381, 161–168.

Coehlo, A.A. and Cheary, R.W. (1997) X-ray line profiling program, XFIT. Internet distributed freeware. Available from site http://www.ccp14.ac.uk.

Hofmeister, A.M. (1997) IR spectroscopy of alkali halides at very high pressures: calculation of equations of state and the response of bulk moduli to the B1-B2 phase transition. Physical Review B, 56, 5835–5855.

Holland, T.J.B. and Redfern, S.A.T. (1997) Unit cell refinement from powder diffraction data: the use of regression diagnostics. Mineralogical Magazine, 61, 65–77.

Johnson, M.C., Walker, D., Clark, S.M., and Jones, R.L. (2001) Thermal decomposition of rhombohedral $KClO_3$ from 29–76 kilobars and implications for the molar volume of fluid oxygen at high pressures. American Mineralogist, 86, 1367–1379.

Nacken, R. (1918) Über die grenzen der mischkristallbildung zwischen kaliumchlorid und natriumchlorid. Sitzungsberichte der Preussischen Akademie der Wissenschaften, Physikalisch-Mathematische Klasse, 192–200.

Newton, R.C. and Wood, B.J. (1980) Volume behavior of silicate solid solutions. American Mineralogist, 65, 733–745.

Reichmann, H.J., Jacobsen, S.D., Mackwell, S.J., and McCammon, C.A. (2000) Sound wave velocities and elastic constants of magnesiowüstite using gigahertz interferometry. Geophysical Research Letter, 27, 799–802.

Skinner, B.J. (1966) Thermal expansion. In S.P. Clark Jr., Ed., Handbook of Physical Constants, Geological Society America Memoir 97, 75–96.

Thompson, J.B. Jr. and Waldbaum, D.R. (1969) Analysis of the two-phase region halite-sylvite in the system NaCl-KCl. Geochimica Cosmochimica Acta, 33, 671–690.

Vaidya, S.N. and Kennedy, G.C. (1971) Compressibility of 27 halides to 45 kbar. Journal of Physics and Chemistry of Solids, 32, 951–964.

Walker, D., Clark, S.M., Jones, R.L., and Cranswick, L.M.D. (2000) Rapid methods for the calibration of solid state detectors. Journal of Synchrotron Radiation, 7, 18–21.

Walker, D., Clark, S.M., Cranswick, L.M.D., Johnson, M.C., and Jones, R.L. (2002a) O_2 volumes at high pressure from $KClO_4$ decomposition: D" as a siderophile element pump instead of a lid on the core. Geochemistry, Geophysics, Geosystems, 3, 11, 1070 (26 pages) Doi: 10.1029/2001GC000225.

Walker, D., Cranswick, L.M.D., Verma, P.K., Clark, S.M., and Buhre, S. (2002b) Thermal equations of state for B1 and B2 KCl. American Mineralogist. 87, 805–812.

Yagi, T. (1978) Experimental determination of thermal expansivity of several alkali halides. Journal of Physics and Chemistry of Solids, 39, 563–571.

Manuscript received January 8, 2002
Manuscript accepted September 9, 2003
Manuscript handled by Robert Dymek